High-spin states in ^{39}K from ^{24}Mg(^{18}O, $p2n\gamma\gamma\cdots$)^{39}K†

J. J. Kolata, Ph. Gorodetzky,* J. W. Olness, A. R. Poletti,‡ and E. K. Warburton
Brookhaven National Laboratory, Upton, New York 11973
(Received 19 October 1973)

The electromagnetic decays of several high-spin states in ^{39}K were studied via heavy-ion-induced reactions involving ^{18}O and ^{19}F bombardments of targets of ^{24}Mg, ^{26}Mg, and ^{27}Al. The ^{39}K states were formed most strongly in the ^{24}Mg(^{18}O,$p2n\gamma\gamma\cdots$)^{39}K reaction which provided the main body of quantitative evidence we report. The identification of specific transitions in ^{39}K, and the resultant decay scheme, are based on Ge(Li) γ-γ coincidence spectra and also on γ-ray yield curves measured for $20 \leq E_B \leq 61$ MeV. Lifetimes of ^{39}K states were measured by the recoil distance method. These lifetimes together with γ-ray angular distributions restrict the allowable spin-parity assignments and multipole mixing ratios for the transitions studied. Arguments based on the proposed reaction mechanism are invoked to give a most probable decay scheme for the high-spin states involved. The resulting data provide new information on the high-spin structure of ^{39}K and also illustrate the power of these heavy-ion-induced compound-nucleus reactions as spectroscopic tools for the investigation of high-spin states in light nuclei.

[NUCLEAR REACTIONS ^{24}Mg(^{18}O,$p2n\gamma\gamma\cdots$), E = 20–61.5 MeV; $\sigma(E,E_\gamma)$, $\gamma\gamma$ coin; deduced ^{39}K levels, tabulated and identified 120 γ rays from ^{24}Mg + ^{18}O at 40 MeV; measured $\sigma(E_\gamma,\theta)$, $T_{1/2}$ for ^{39}K transitions; deduced Λ for transitions and J^π, δ for high-spin ^{39}K levels.]

I. INTRODUCTION

Heavy-ion-induced compound-nuclear reactions have proved to be valuable spectroscopic tools in the investigation of high-spin states in heavy nuclei ($A > 100$).[1] In this mass region and at tandem Van de Graaff energies, the predominant decay of the compound nucleus is via multineutron evaporation processes so that the reactions observed are of the type (HI, $xn\gamma\gamma\cdots$) where x is a small positive integer whose value is highly correlated with the incident beam energy. In the last few years, this type of reaction has been extended with some success to the investigation of lighter-mass nuclei ($A < 30$).[2] Because of the lower Coulomb barrier for compound nuclei in this mass region, charged-particle emission can compete favorably with neutron emission so that several final nuclei are formed with comparable probabilities at any given bombarding energy. The problem of identifying the observed γ rays with a particular nucleus is accordingly more severe but, as we shall see, the usefulness of this type of reaction in the investigation of high-spin states is not impaired. The present work results from a program recently initiated at Brookhaven National Laboratory (BNL) to study high-spin states in nuclei in the upper portion of the $2s$-$1d$ shell and the lower part of the $1f$ shell. Beams of ^{14}N, ^{16}O, ^{18}O, and ^{19}F ions with energies of 20–60 MeV from either of the two BNL MP-tandem accelerators have been used to bombard targets of ^{24}Mg, ^{26}Mg, ^{27}Al, and ^{28}Si. We report here on states observed in ^{39}K as an illustration of the type of information which can be obtained from γ-ray spectroscopy in heavy-ion-induced reactions.

The properties of low-lying high-spin states in ^{39}K resulting from the $(d_{3/2})^{-2}$–$f_{7/2}$ configuration have been predicted in the shell model.[3,4] Similar sets of states have been calculated[5,6] in weak-coupling models based on a $d_{3/2}$ proton hole coupled to the 3^- and 5^- states of ^{40}Ca. Decay schemes, mixing ratios, and lifetime limits for the two lowest-lying high-spin states at 2814 and 3598 keV have been known for some time.[7,8] Accurate lifetime information[9,10] has only recently become available for them. We shall assume spin-parity assignments of $\frac{7}{2}^-$ and $\frac{9}{2}^-$ for these two states, respectively, although, as concluded in the recent critical review of Endt and Van der Leun,[11] the spin assignments are not rigorous but only strongly circumstantial. Assignments of $(\frac{7}{2}^-, \frac{9}{2}^-, \frac{11}{2}^-)$ have been proposed for the high-spin members of two doublets at 3.94 and 4.52 MeV,[12] while Endt and Van der Leun conclude the weaker $J = \frac{5}{2}$–$\frac{11}{2}$ for both. The present paper reports additional information on the electromagnetic decay modes of the 2.81-, 3.60-, and 3.94-MeV states. Two new high-spin states at 5.72 and 6.48 MeV are also identified and their decay modes are presented.

II. EXPERIMENTAL PROCEDURE

A variety of experimental methods was used in the process of identifying the observed γ-ray

transitions and measuring the electromagnetic decay properties of the associated nuclear states. The identification problem was moderately severe as illustrated in Fig. 1, which shows a singles γ-ray spectrum for the $^{18}O+^{24}Mg$ reaction taken at a beam energy of 40.0 MeV. The 119 γ-ray lines visible in this spectrum are associated in Table I with the nuclei in which the transitions occur. Seven of the γ-ray lines in Fig. 1 are identified with the $^{24}Mg(^{18}O, p2n\gamma\gamma\cdots)^{39}K$ reaction. The identifications of Table I are based on excitation functions, γ-γ coincidence data, and γ-ray energy measurements for the six reactions from ^{18}O and ^{19}F beams on ^{24}Mg, ^{26}Mg, and ^{27}Al targets. The energies quoted for the 119 γ rays are the averages of the values observed in these six reactions. In particular, the ^{39}K γ rays were observed in the reactions $^{24}Mg(^{18}O, p2n)^{39}K$, $^{27}Al(^{18}O, \alpha 2n)^{39}K$, and $^{26}Mg(^{19}F, \alpha 2n)^{39}K$, but not in the $^{18}O+^{26}Mg$, $^{19}F+^{24}Mg$, or $^{19}F+^{27}Al$ reactions.

The first experiment performed to identify the γ-ray transitions was a thin-target excitation function measurement. Targets of isotopically separated ^{24}Mg (>99%) were evaporated to a thickness of 150 $\mu g/cm^2$ onto thick W backings and bombarded with an ^{18}O beam from one of the BNL MP-tandem accelerators. The beam current was typically 150 nA of 5^+ ^{18}O ions, and the beam energy was varied from 20 to 61 MeV in steps of 5 MeV. Typical excitation functions for several γ-ray lines are shown in Fig. 2 and the results are summarized for all transitions in Table I. The excitation functions for γ-ray transitions in ^{39}K were all very similar as expected. The average intensity of five transitions from the three lowest ^{39}K states populated in the $^{24}Mg(^{18}O, p2n)^{39}K$ reaction, arbitrarily normalized to unity at 45 MeV, is shown in the left half of Fig. 2, with error bars representing the rms spread of the individual measurements about the average value. Individual

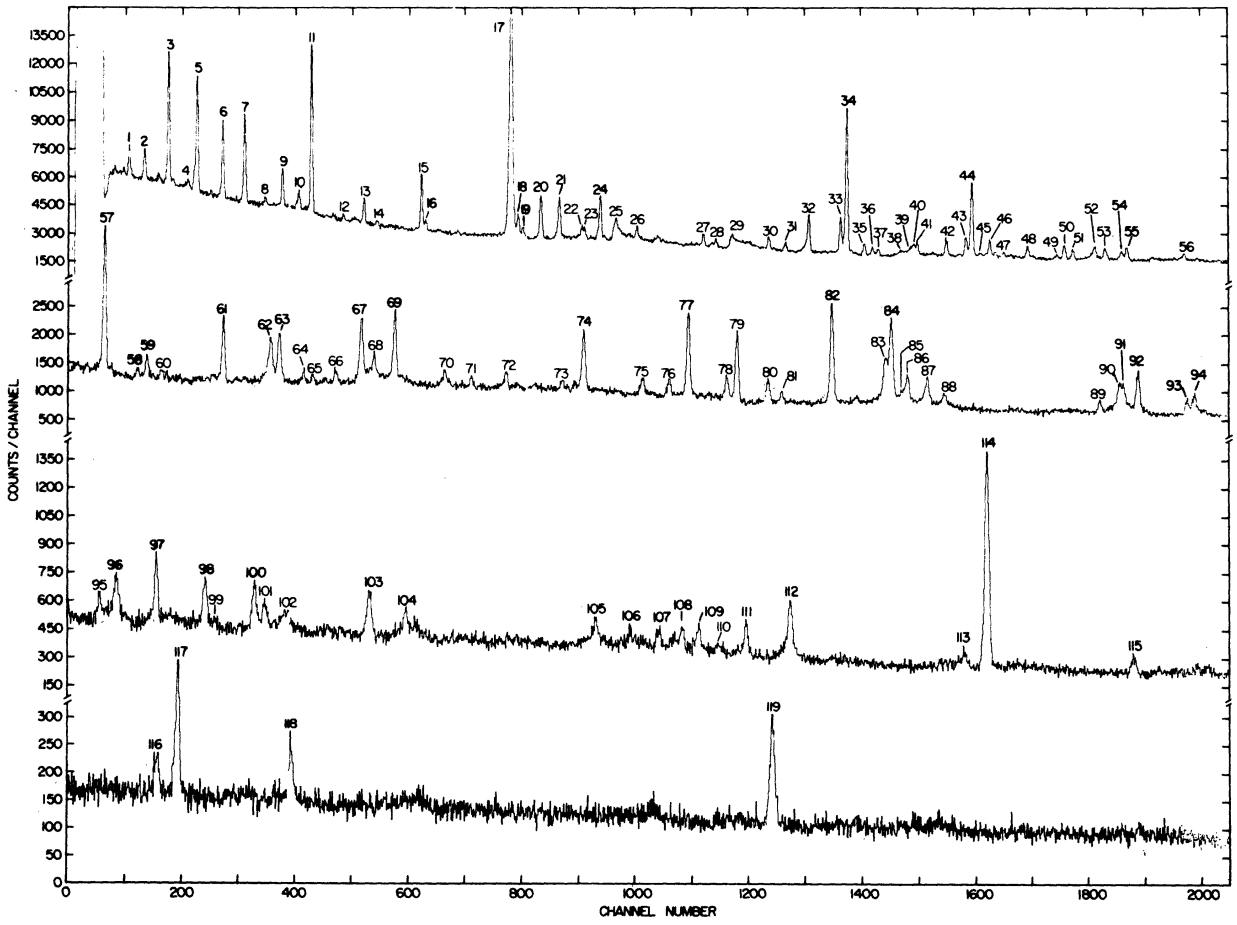

FIG. 1. γ-ray spectrum from $^{18}O+^{24}Mg$ at $E(^{18}O)=40.0$ MeV. The 119 γ-ray lines indicated are identified in Table I. Note that the channel numbers shown apply only to the uppermost of the four quarters of the spectrum shown, and increase by 2048 channels for each succeeding quarter. The dispersion is 0.465 keV/channel.

TABLE I. γ rays observed from ^{18}O+^{24}Mg at 40 MeV. Key: C, used for energy calibrations; B, from Coulomb excitation of the *W* backing; T, from one- or two-nucleon transfer reaction; I, from a target impurity of either ^{26}Mg or ^{27}Al, or from room background; N, the energy is nominal, i.e., $\pm\sim 1$ keV; U, unknown; CE, Coulomb excitation; SE, single escape; DE, double escape; ?, questionable assignment; R, the yield is still rising at 61.5 MeV; H, the yield has leveled off at 61.5 MeV.

No.	E_γ (keV)	Identification	Excitation[a] function
1	197.147(12)	^{19}F(C, T)	R
2	209.70(10)	^{183}W(B)	R
3	229.317(8)	^{182}W(C, B)	R
4	245.25(30)	^{183}W(B)	R
5	252.84(10)	^{184}W(C, B)	R
6	273.84(10)	^{186}W(B)	R
7	291.76(10)	^{183}W(B)	R
8	308.57(15)	^{38}Cl	R
9	322.80(15)	^{37}Ar	45(27)
10	336.19(10)	^{40}K	38(21)
11	346.69(10)	^{39}K(C)	46(23)
12	372.81(5)	^{43}Ca(C, I)	
13	389.71(15)	^{25}Mg(T)	R
14	400.30(40)	U	
15	437.04(8)	^{42}Ca(C, I)	43(21)
16	440.83(20)	^{42}K(I)	
17	511.006(5)	Ann. Rad. (C)	
18	516.8(N)	^{40}K(?)	
19	521.30(30)	^{37}Ar	44(?)
20	535.91(10)	^{37}Cl	44(24)
21	551.08(10)	^{39}Ar(?)	47(24)
22	569.90(50)	U	
23	572.00(20)	^{42}K(I)	
24	584.94(10)	^{25}Mg(T) + ^{208}Pb(I)	R
25	597.90(50)	^{74}Ge(n,$n'e$) + ^{37}Ar	
26	615.38(20)	^{186}W(B)	R
27	669.87(8)	^{38}Ar(C)	R
28	680.22(30)	U	R
29	692(N)	Ge(n,$n'e$)	
30	724.44(15)	^{37}Cl	43(23)
31	738.09(15)	^{186}W(B)	R
32	757.19(12)	^{39}K	48(27)
33	783.50(15)	^{39}K(C)	46(25)
34	788.44(10)	^{36}Cl	H
35	803.09(10)	U	
36	809.88(12)	^{42}Ca(I)	45(27)
37	814.75(15)	^{42}Ca(I)	45(?)
38	834.5(N)	U	
39	840.1(N)	U	
40	843.74(3)	^{27}Al(I, C, CE)	R
41	846.99(10)	^{56}Fe(?)	
42	870.83(15)	^{17}O(T)	R
43	886.5(N)	U	50(16)
44	891.57(10)	^{40}K(C)	38(20)
45	897.88(50)	U	
46	906.22(30)	^{37}Cl	43(25)
47	917.87(12)	^{42}Ca(I)	
48	937.67(25)	^{37}Ar	45(23)
49	961.74(30)	U	
50	967.85(30)	U	H
51	974.82(15)	^{25}Mg(T)	H
52	992.38(30)	^{39}Ar(?)	47(35)
53	1001.34(20)	^{34}S(?)	48(35)
54	1014.44(4)	^{27}Al(I, C, CE)	53(37)
55	1018.95(50)	U	H
56	1065.80(N)	U	48(23)
57	1130.03(12)	^{39}K	46(24)
58	1157.50(15)	^{43}Sc(I, C)	
59	1165.04(20)	U	
60	1176.81(50)	U	
61	1227.66(8)	^{42}Ca(I, C)	43(21)
62	1266.72(25)	U	48(30)
63	1273.53(10)	U	R
64	1293.64(4)	^{41}K(C)	
65	1301.22(50)	^{39}Cl(?)	
66	1320.19(40)	U	
67	1340.82(20)	^{39}Ar(?)	46(27)
68	1351.63(20)	U	~45(~15)
69	1368.54(4)	^{24}Mg(C, CE)	H
70	1409.84(40)	U	
71	1431.66(20)	^{40}Ar	
72	1460.90(20)	^{40}Ar	36(29)
73	1506.96(20)	^{37}Ar	
74	1524.58(8)	^{42}Ca(C, I)	43(23)
75	1573.57(30)	^{37}Ar	45(28)
76	1595.40(30)	U	>45(>30)
77	1611.24(9)	^{37}Ar(C)	44(26)
78	1642.42(10)	^{38}Ar(C)	R
79	1651.24(10)	^{40}K(C)	38(19)
80	1676.97(40)	^{41}K + ^{43}Ca(I)	
81	1688.35(50)	U	
82	1729.75(20)	^{36}Cl	H
83	1774.07(12)	^{39}K	50(26)
84	1778.81(9)	^{28}Si(I, T, C)	R
85	1788.0(N)	U	
86	1791.76(40)	^{39}K(2814 DE)	45(24)
87	1808.66(7)	^{26}Mg(T, C)	H
88	1822.65(30)	^{38}Ar	
89	1950.73(50)	U	
90	1967.11(50)	U	
91	1970.55(50)	U	
92	1982.00(20)	^{18}O(CE)	R
93	2022.17(50)	U	
94	2028.28(30)	U	H
95	2081.17(40)	^{37}Cl(3103 DE)	
96	2094.87(70)	^{37}Ar	42(20)
97	2127.41(40)	^{34}S	46(27)
98	2167.53(5)	^{38}Ar(C)	R
99	2175.34(N)	3197 DE	
100	2208.23(60)	U	45(19)
101	2216.81(30)	^{37}Ar	
102	2234.5(N)	U	R
103	2302.88(50)	^{39}K(2814 SE) + ^{42}Ca(I)	45(19)
104	2332.57(40)	U	
105	2490.29(40)	U	48(29)
106	2518.68(80)	U	
107	2542.61(40)	U	
108	2561.61(80)	^{34}S(?)	45(?)

TABLE I *(Continued)*

No.	E_γ (keV)	Identification	Excitation [a] function	No.	E_γ (keV)	Identification	Excitation [a] function
109	2575.25(25)	^{39}K(C, 3597 DE)		115	2935.08(80)	U	R
110	2592.4(N)	^{37}Cl(3103 DE)		116	3086.18(50)	^{37}Cl + ^{39}K(3597 SE)	
111	2614.47(10)	^{208}Pb(I, C)		117	3103.40(20)	^{37}Cl(C)	45(25)
112	2651.02(25)	^{39}Ar(?)	48(27)	118	3197.34(40)	U	47(22)
113	2795.31(40)	^{39}Ca + ^{37}Ar(?)	H	119	3597.25(25)	^{39}K(C)	44(22)
114	2814.24(20)	^{39}K(C)	44(22)	120	4009.62(N)	^{37}Cl	

[a] EMAX(FWHM) ≡ the energy of maximum yield (±2 MeV) and the full-width-at-half-maximum of the yield curve (±4 MeV).

excitation functions for transitions from the two highest-energy ^{39}K states are also shown to illustrate the slight tendency, observed in previous work,[13] for the peak of the excitation function to shift toward higher beam energies as the excitation energy of the γ-ray emitting state increases. Excitation functions for γ-ray transitions in other nuclei are shown for comparison purposes in the right half of Fig. 2. The *np* evaporation process shows a characteristic peak at about 38 MeV with a full width at half maximum (FWHM) of 19 MeV, while the excitation function for the other two-particle evaporation process illustrated (αp) is substantially broader and is also shifted upward so that the peak occurs at about 44 MeV. Similarly, the αnp excitation function is broader than

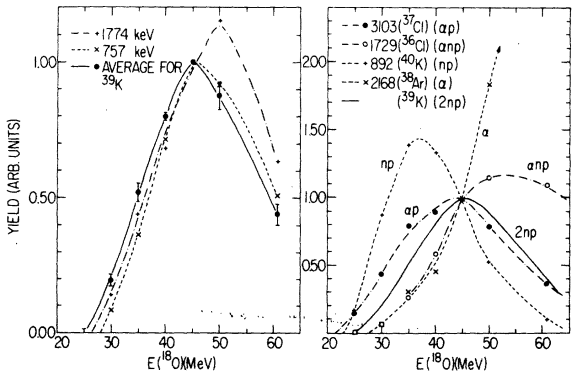

FIG. 2. Excitation function for selected γ rays from ^{18}O + ^{24}Mg. Results for ^{39}K are displayed in the left half: the dots show the average intensity of five γ-ray transitions from the three lowest-lying states in ^{39}K, with error bars representing the rms spread of the individual measurements. Also shown are excitation functions for the two remaining γ-ray transitions in ^{39}K. Similar data for outgoing channels leading to other final nuclei are shown for comparison on the right. It should be noted that each excitation function is arbitrarily normalized to unity at $E(^{18}O) = 45$ MeV. All of the curves in this figure are drawn only to guide the eye. Unless noted, error bars are smaller than the data points.

that of the *p2n* three-particle evaporation process, and its peak is also shifted upward, this time by about 15 MeV. The excitation function for single-α-particle emission (Fig. 2) does not display the typical bell shape expected for evaporation from a compound nucleus. The rapid and sustained rise of the formation probability for ^{38}Ar well beyond the expected peak for single-nucleon evaporation processes possibly indicates a large contribution from direct-reaction mechanisms to the ^{18}O(^{24}Mg, α)^{38}Ar reaction.

The second experiment to identify the γ-ray lines shown in Fig. 1 was a γ-γ coincidence measurement performed at 40-MeV beam energy. Two Ge(Li) detectors with active volumes of 60 and 70 cm^3 were positioned 4 cm from a thick target of natural Mg metal at 0 and 90° to the incident beam. This choice of detector angles allowed the easy observation of Doppler effects while minimizing the chance that a γ ray might be overlooked due to strong spatial correlation effects. Coincident events were determined within a time gate of 60 ns using conventional electronic circuitry, and the two associated γ-ray energy signals were each digitized into 4096 channels and stored on magnetic tape for later analysis. In addition, selected portions of this 4096 × 4096 coincidence matrix were displayed on line in a 2048 × 16 array as a monitor of the quality of the coincidence data. Finally, a gate signal associated with random coincidences was also generated so that a spectrum of random events was collected simultaneously with the true coincidences.

In the playback of these data tapes, the random and real-plus-random spectra in one of the detectors associated with energy gates set around selected γ-ray lines in the other detector were recorded, and the randoms were subsequently subtracted from the real-plus-random spectra. In addition, it was necessary to account for the true coincidences with Compton events from higher-energy γ rays which happen to fall within the selected energy gates. This was done by setting an

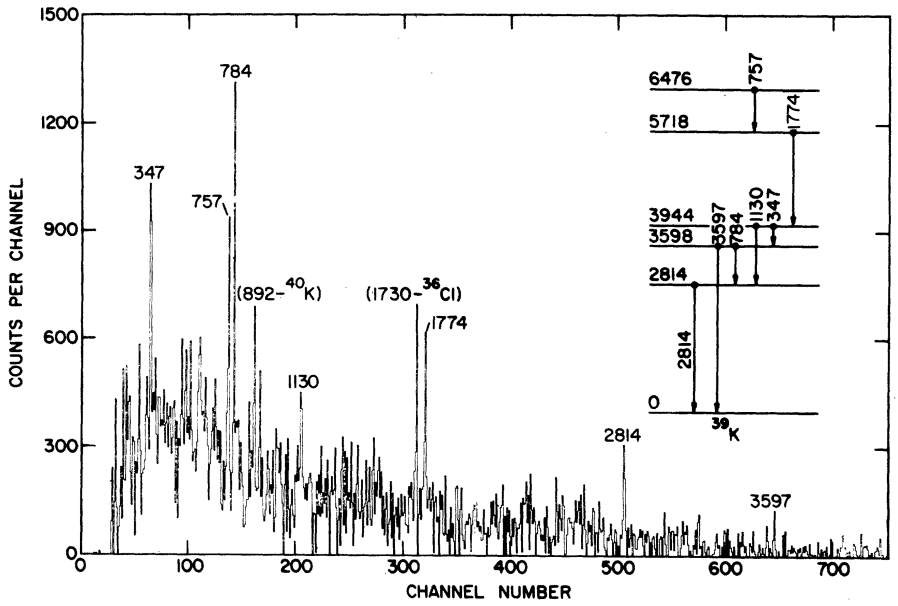

FIG. 3. Coincidence spectrum for ^{39}K γ rays. This data is a sum of several coincidence gates and shows all the observed transitions in ^{39}K. Transitions are identified according to transition energy (in keV). The inset level scheme shows their placement in ^{39}K. Two contaminant γ-ray lines from transitions in other nuclei are also identified.

additional gate as close as possible to each of the selected peaks and subtracting the resultant Compton coincidence spectrum in order to generate a final corrected spectrum. The entire process was subsequently repeated with the roles of the two detectors interchanged.

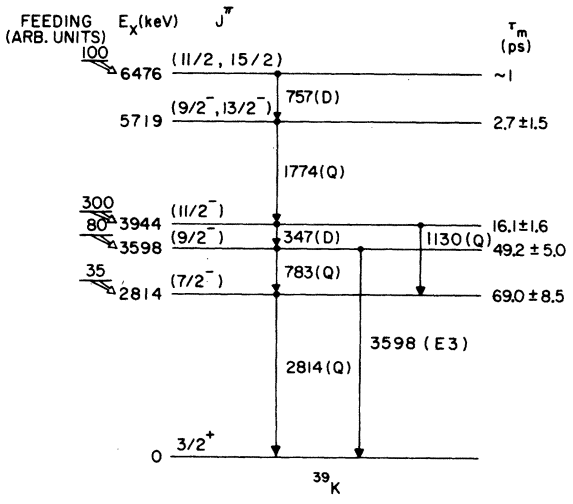

FIG. 4. Decay scheme for ^{39}K states observed in this experiment. The γ transitions are labeled with their predominant character ($D \equiv$ dipole, $Q \equiv$ quadrupole, $E3 \equiv$ electric octupole). The mean lifetimes for all states and the spin assignments to the three highest-energy states are from the present experiment. Finally, the side feeding into each of these states from the ^{18}O + ^{24}Mg reaction at 40.0 MeV is also shown.

A coincidence spectrum for ^{39}K γ rays is shown in Fig. 3. This spectrum is actually the sum of several coincidence gates and shows all the γ-ray lines associated with transitions in ^{39}K. The decay scheme deduced from these data is shown in Fig. 4. Aside from a possible interchange of the upper two transitions, this decay scheme is the only one which is consistent with the observed coincidence spectra.

After the γ rays corresponding to transitions in ^{39}K were isolated and identified, the task of measuring the electromagnetic decay modes of the nuclear states could be begun. We relied heavily here on one of the most outstanding characteristics of these heavy-ion-induced reactions: the fact that the residual nuclei are very strongly aligned with respect to the beam axis.[1] It is therefore possible to obtain data on the multipolarities, and even at times the mixing ratios, of the γ-ray transitions in these nuclei from a measurement of their angular distributions. In some cases the conclusions are rigorous and in other cases they depend on assumptions about transition strengths or the reaction mechanism of the heavy-ion reaction. We will differentiate between these cases in the following discussion.

The angular distribution measurements were made with the 60-cm^3 Ge(Li) detector placed at a distance of 13 cm from the target, which was the same target used for the excitation function ex-

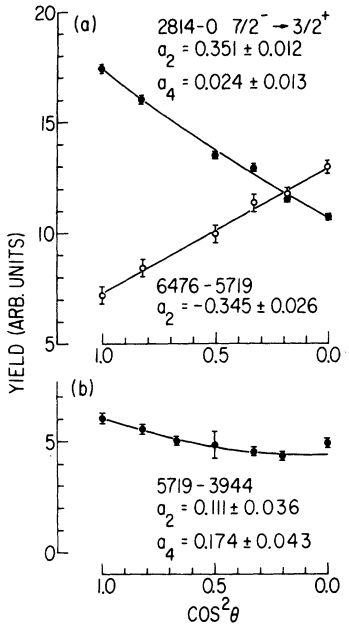

FIG. 5. Angular distributions for three of the γ-ray transitions in ^{39}K from ^{18}O+^{24}Mg at 40.0 MeV. The curves shown are the fits to the data discussed in the text. The resulting coefficients of the Legendre polynomials are also shown.

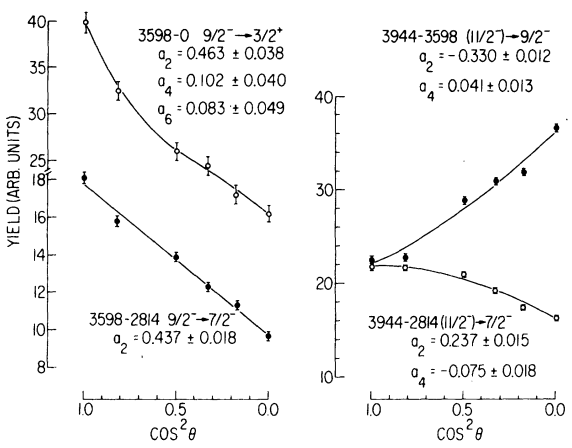

FIG. 6. Angular distributions for the four remaining γ-ray transitions in ^{39}K. The notation is that of Fig. 5.

periment. The other Ge(Li) detector was fixed in position at 90° to the beam and at 11 cm from the target. Selected γ-ray lines in this monitor detector were used to normalize the spectra from the movable counter, which were taken at seven angles ranging from 0 to 90° relative to the beam direction. The experimental angular distributions for transitions in ^{39}K, shown in Figs. 5 and 6, were fit to the functional form

$$W(\theta) = A_0[1 + a_2P_2(\theta) + a_4P_4(\theta) + a_6P_6(\theta)] .$$

The coefficients of the Legendre polynomials, corrected for the finite size of the γ-ray detector, are listed in Table II and also in Figs. 5 and 6. The quoted errors are purely statistical (standard deviation) and do not include possible contributions from systematic errors in the positioning of the detectors, which are estimated to be less than 5%.

TABLE II. Transitions in ^{39}K observed from ^{24}Mg+^{18}O.

Transition [a] E_i (keV)	E_f (keV)	E_γ (keV)	J^π_i	J^π_f	Multipolarity [b]	τ initial level [c] (ps)	Angular distribution coefficients [d,e] a_2(%)	a_4(%)	a_6(%)	χ^2
6475.69(29)	5718.49	757.19(12)	$(\frac{11}{2}, \frac{15}{2})$	$(\frac{9}{2}^-, \frac{13}{2}^-)$	($E1$,$M1$)	$1.0 \lesssim \tau < 3.0$	−34.5±2.6	0	0	0.3
5718.49(26)	3944.38	1774.07(12)	$(\frac{9}{2}^-, \frac{13}{2}^-)$	$(\frac{11}{2}^-)$	($M1$)	2.7±1.5	11.1±3.6	17.4±4.3	0	0.8
3944.38(23)	3597.65	346.69(10)	$(\frac{11}{2}^-)$	$\frac{9}{2}^-$	$M1$	16.1±1.6	−33.0±1.2	4.1±1.3	0	7.3
3944.38(23)	2814.35	1130.03(12)	$(\frac{11}{2}^-)$	$\frac{7}{2}^-$	$E2$		23.7±1.5	−7.5±1.8	0	1.9
3597.65(25)	2814.35	783.50(15)	$\frac{9}{2}^-$	$\frac{7}{2}^-$	$M1$	49.2±5.0	43.7±1.8	0	0	1.3
3597.65(25)	0	3597.25(25)	$\frac{9}{2}^-$	$\frac{3}{2}^+$	$E3$		46.3±3.8	10.2±4.0	8.3±4.9	0.5
2814.35(20)	0	2814.24(20)	$\frac{7}{2}^-$	$\frac{3}{2}^+$	$M2$	69.0±8.5	35.1±1.2	2.4±1.3	0	2.5

[a] The excitation energies are derived from recoil-corrected γ-ray energies.

[b] Lowest allowed multipole. The 3598→2814 transition goes primarily by $E2$. See the text for further discussion.

[c] Mean lifetime of the initial state measured in the present experiment.

[d] A zero entry for a_4 or a_6 implies that the associated term $P_i(\theta)$ was not included in the fit. The measured a_4 or a_6 coefficients were consistent with zero in these cases.

[e] The theoretical coefficients for full alignment and the indicated pure multipolarities are in the range $a_2 = +(45-51)$, $a_4 = -(24-38)$ for quadrupole transitions and $a_2 = -(17-33)$ for dipole transitions.

The last experimental technique employed was the recoil-distance method (RDM) for measuring the lifetimes of nuclear states.[14] This technique exploits the fact that the recoil velocities of residual nuclei resulting from heavy-ion-induced reactions are large. In this series of measurements, the target was a 300-μg/cm^2 film of ^{24}Mg evaporated onto a 1.1-mg/cm^2 Ni foil which was subsequently stretched flat and placed into a RDM apparatus.[15] The 60-cm^3 Ge(Li) detector was placed at 0° to the beam axis, and γ-ray spectra were acquired with the gold recoil-ion stopper at 10 distances between 0.03 and 1.78 mm from the target. The beam energy was 40 MeV. Typical spectra showing the "stopped" peak (intensity I_0) and the "shifted" peak (intensity I_s) for several transitions are shown in Fig. 7. The intensities of these peaks were extracted and corrected for: (1) the change in efficiency of the Ge(Li) detector as a function of γ-ray energy, (2) the change in the solid angle subtended by the detector due to changes in the stopper distance, (3) the change in the effective solid angle subtended by the detector due to the conversion from the center-of-mass coordinates of the moving ion to the laboratory system, and (4) the spread in velocity of the recoiling nuclei. The corrected ratios $I_0/(I_0+I_s)$ were then formed and are shown in Figs. 8 and 9 for the transitions in ^{39}K. For some of these transitions, it was not possible to normalize to (I_0+I_s) as discussed below and we therefore used the corrected total yield $I_n=I_0+I_s$ for the 1130-keV transition. The error bars shown in Figs. 8 and 9 are purely statistical (standard deviation). An estimated uncertainty of ±2.5 μm was assigned to the relative distance settings.

The average axial velocity of the recoil ions, $\bar{v}/c=0.0277\pm0.0002$, was determined from the energy differences between the stopped and shifted peaks. The data of Figs. 8 and 9 were for the most part fitted to the analytical form given in Ref. 10 in the case where the state of interest is fed partially from a higher-lying state which has

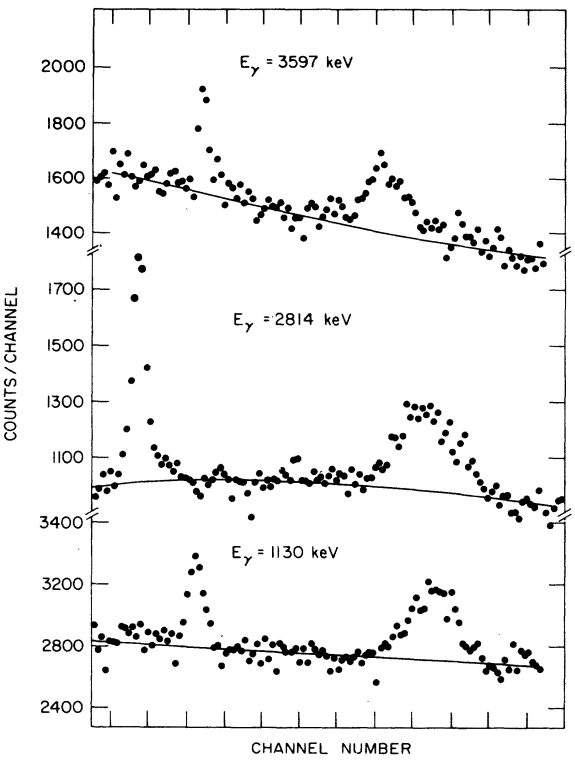

FIG. 7. Portions of γ-ray spectra observed in the RDM measurements. The narrow "stopped" peak and broadened "shifted" peak for several transitions are shown. The stopper was at a distance of 0.767 mm for the 3597- and 2814-keV transitions, and at 0.178 mm for the 1130-keV transition. The dispersions (top-to-bottom) are 2.076-, 1.038-, and 0.519-keV/channel.

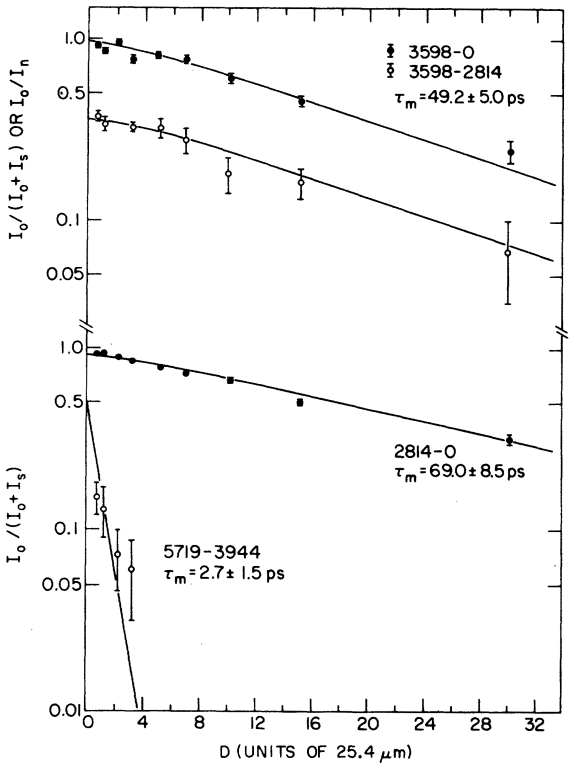

FIG. 8. Corrected normalized intensity ratios as a function of stopper distance for four transitions in ^{39}K. The normalizing factor I_n, which applies only to the 3598-2814 transition, is the corrected sum (I_0+I_s) for the 1130-keV transition (see text). The mean lifetimes shown are those obtained from the fit to the data illustrated by the solid curves. The 6476-5719 transition (not shown) had a measurable stopped peak I_0 only at the closest distance (17.8 μm), corresponding to a lifetime of about 1 ps.

itself a lifetime comparable to that of the state being investigated. The feeding ratios were estimated from the relative populations and branching ratios determined in the recoil-distance and angular-distribution experiments. The data for the 1130-keV transition were used to determine the correction D_0 to the distances measured relative to the nominal zero position. This correction was $D_0 = -25.4 \pm 7.6\ \mu\text{m}$.

The decay of the 2814-keV level is more complicated since it is fed from two states, one of which is itself fed from above. In this case, the formula for the ratio $I = I_0/(I_0 + I_s)$ as a function of time is

$$
\begin{aligned}
I = {} & A_0 f_{AC}\left(\frac{\tau_C}{\tau_A - \tau_C}\right)\left(\frac{\tau_A}{\tau_C}e^{-t/\tau_A} - e^{-t/\tau_C}\right) \\
& + B_0 f_{BC}\left(\frac{\tau_C}{\tau_B - \tau_C}\right)\left(\frac{\tau_B}{\tau_C}e^{-t/\tau_B} - e^{-t/\tau_C}\right) + C_0 e^{-t/\tau_C} \\
& + C_0 f_{AB} f_{BC}\left[\left(\frac{\tau_A}{\tau_A - \tau_C}\right)\left(\frac{\tau_A}{\tau_A - \tau_B}\right)e^{-t/\tau_A}\right. \\
& + \left(\frac{\tau_B}{\tau_B - \tau_C}\right)\left(\frac{\tau_B}{\tau_B - \tau_A}\right)e^{-t/\tau_B} \\
& \left. + \left(\frac{\tau_C}{\tau_C - \tau_A}\right)\left(\frac{\tau_C}{\tau_C - \tau_B}\right)e^{-t/\tau_C}\right],
\end{aligned}
$$

where (1) A_0 and B_0 are the initial populations of the states feeding the level C; (2) f_{AB} is the fraction of the nuclei in state A that decay to state B with similar definitions for f_{AC} and f_{BC}, and (3) τ_A, τ_B, and τ_C are the mean lifetimes of the states in question. This equation, when converted to distance using $D = \bar{v}t$, is somewhat simplified from the equivalent form for the two-level decay[9] because it does not include the correction to the decay resulting from the varying solid angle subtended by the detector as the stopper is moved.

The mean lifetimes for the five states in ^{39}K determined from the present experiment are shown in Figs. 8 and 9 and are also listed in Table II. The uncertainties include the statistical errors as well as an estimate of various systematic uncertainties discussed below for each individual transition. The fastest γ-ray transition observed in ^{39}K has a measured mean life of the order of 1 ps, which we take to be the upper limit on the "feeding time", i.e., the time it takes for the compound nucleus to decay to the first observed γ-emitting level. Actually, there is evidence in this same data (for states in ^{37}Ar) and in data from other reactions[13] (for states in ^{41}Ca and ^{41}K) that the feeding times are substantially less than 1 ps. That is, we observe in these reactions Doppler-shifted γ transitions which correspond to lifetimes of less than 1 ps.

III. RESULTS AND DISCUSSION

In this section we discuss the transition strengths and spin-parity assignments which can be deduced from the present data for the five states in ^{39}K we have investigated. For the most part, the spin assignments are based on the model-dependent assumption that the initial γ-emitting states are highly aligned. The angular momentum brought in by the incident heavy ion in these reactions (generally $> 25\hbar$) is much larger than any other angular momentum vectors involved in the reaction. For this reason, one expects nearly complete initial alignment of the compound nucleus relative to the beam direction, i.e., population of the lowest m substate(s) only. This alignment will be reduced in the subsequent evaporation of a few nucleons to reach the final γ-emitting nucleus. However, again because of the very large incident angular momentum, it is reasonable to suppose that the substate populations (which in general depend on the detailed formation process of the final nucleus) can be represented by a distribution function of one parameter. It has been shown for heavier nuclei that a Gaussian distribution of substates simulates rather well the experimental

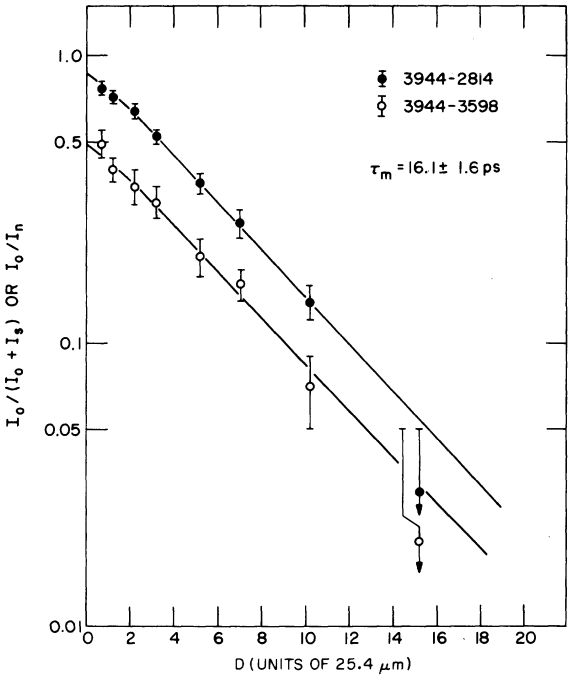

FIG. 9. Corrected normalized intensity ratios for the two transitions from the ^{39}K 3944-keV state. The normalizing factor I_n, which applies only to the 3944-3598 transition, is the corrected sum $(I_0 + I_s)$ for the 1130-keV transition (see text). The mean lifetime shown was obtained from the fits to the data shown by the solid curves.

γ-ray angular distributions in heavy-ion reactions.[16] In the following discussion, we will assume that a single-parameter distribution function, not necessarily Gaussian, is all that is necessary to describe the substate populations. This is not a rigorous argument so that our spin assignments are to some extent model dependent and will therefore be enclosed in parentheses.

A. Decay of the 2814-keV state

The lifetime of this level has been previously measured by the RDM[9] and with comparable accuracy by the attenuated Doppler-shift method[11] using a gas target. There is reasonably good agreement between the present mean life ($\tau = 69.0 \pm 8.5$ ps) and those of Ref. 9 (79 ± 8 ps) and Ref. 10 (63 ± 10 ps). Bond and Kern neglected the feeding from the 3944-keV level which, if it were included, would tend to reduce their measured mean life by a small amount.[17]

The 2814-keV state decays to the ground state by a mixed $M2/E3$ transition. Since the side feeding into this state is less than 10% of its total population (Fig. 4), and since the alignment of the two states feeding it has been measured (see below), it is possible to compute the mixing ratio for the transition from the experimental a_2 coefficient.[18] We define the attenuation coefficient[19] α_K in terms of the Legendre polynomial coefficients a_K as

$$a_K = \alpha_K a_K^{\max},$$

where $a_K^{\max}$ is the correlation coefficient for complete alignment in the $m = \pm\frac{1}{2}$ substates. Our expectation is that the high degree of alignment provided by the heavy-ion reaction will be retained sufficiently that $0 < \alpha_K < 1$. This is a model-dependent assumption. The alignment computed for the 2814-keV state from the angular distributions of the feeding transitions is $\alpha_2 = 0.45 \pm 0.05$, and the two solutions for the mixing ratio are $x = -0.24 \pm 0.05$ and $x = -6.6 \pm 1.0$. The latter value is rejected since it implies an $E3$ transition of nearly 200 Weisskopf units (W.u.).[20] The first solution is in good agreement with the results of previous angular correlation measurements by Lopes *et al.*[7] ($x = -0.19 \pm 0.10$), and also with the value deduced by Kessel, Bass, and Wechsung[10] from existing inelastic scattering data ($|x| = 0.17 \pm 0.04$). The associated transition strengths (Table III) are quite reasonable[20] and the $E3$ strength is in good agreement with the value of 9 W.u. calculated from the phonon-hole coupling model.[6]

B. Decay of the 3598-keV level

The mean life of this state from the present experiment ($\tau = 49 \pm 5$ ps) is somewhat smaller than the values quoted in Ref. 9 ($\tau = 59 \pm 4$ ps) and Ref. 10 ($\tau = 60 \pm 9$ ps). Here again, inclusion of the neglected feeding from the 3944-keV level would reduce the measured mean life in Ref. 9 by a small amount.[17]

The 3598-keV level decays to both the ground

TABLE III. Branching ratios, mixing ratios, and transition strengths for γ-ray transitions in ^{39}K.

Transition $E_i \rightarrow E_f$ (keV)	J^π_i	J^π_f	Branching [a] (%)	Multipolarity	Multipole [a] mixing ratio, x	$\lvert M\rvert^2$ (W.u.) [b]	Upper limit on $M1$ transition strength [b] (W.u.)
6476 → 5719	$(\frac{11}{2}, \frac{15}{2})$	$(\frac{9}{2}^-, \frac{13}{2}^-)$	100	$E1, M1$	$-0.27 \le x \le 0.10$	$\sim 2\times10^{-3}$ ($E1$); ~ 0.07 ($M1$)	
5719 → 3944 [c]	$(\frac{13}{2}^-)$	$(\frac{11}{2}^-)$	100	$M1$	$-3.7 \le x \le -1.5$	$(2.7 \pm 1.5)\times10^{-4}$	
				$E2$		1.9 ± 1.0	
5719 → 3944 [c]	$(\frac{9}{2}^-)$	$(\frac{11}{2}^-)$	100	$M1$	$2.5 \le x \le 5.7$	$(1.3 \pm 0.7)\times10^{-4}$	4.5×10^{-3}
				$E2$		2.0 ± 1.1	
3944 → 3598	$(\frac{11}{2}^-)$	$\frac{9}{2}^-$	36 ± 5	$M1$	0.16 ± 0.02	$(1.6 \pm 0.3)\times10^{-2}$	2.3×10^{-2}
				$E2$		8.9 ± 1.5	
3944 → 2814	$(\frac{11}{2}^-)$	$\frac{7}{2}^-$	64 ± 5	$E2$	$\cdots$	2.2 ± 0.3	
3598 → 2814	$\frac{9}{2}^-$	$\frac{7}{2}^-$	41 ± 8	$M1$	$-2.3 < x < -0.65$	$(3.0 \pm 0.7)\times10^{-4}$	7.9×10^{-4}
				$E2$		1.3 ± 0.3	
3598 → 0	$\frac{9}{2}^-$	$\frac{3}{2}^+$	59 ± 8	$E3$	$\cdots$	29 ± 5	
2814 → 0	$\frac{7}{2}^-$	$\frac{3}{2}^+$	100	$M2$	-0.24 ± 0.05	0.30 ± 0.04	
				$E3$		10.6 ± 1.3	

[a] Branching and mixing ratios determined in the present experiment. See text for a comparison to previous results for the decay of the 3598- and 2814-keV states.

[b] Present work. The uncertainties were propagated from the errors in the lifetime and branching ratio measurements and do not include uncertainties in the mixing ratio x. Upper limits allow for two standard deviations in the lifetime.

[c] Transition strengths are computed for both possible J^π assignments to the 5719-keV state.

state and the 2814-keV level. The branching ratios determined from the present experiment are (0.59 ± 0.08) and (0.41 ± 0.08), respectively, compared to values of (0.61 ± 0.07) and (0.39 ± 0.07) quoted in Ref. 7. The spin-parity of this state is assumed to be $J^\pi = \frac{9}{2}^-$ as discussed in Sec. I, so that its ground-state decay is $E3$ (29 ± 5 W.u.) with a possible $M4$ admixture. However, the lifetime (Table II) is short enough so that an $M4$ component strong enough to affect the a_2 coefficient in the ground-state decay by 10% would have a strength of 3×10^5 W.u. We can therefore assume a negligible $M4$ component and use the experimental a_2 coefficient (Table II) for the ground-state transition to determine the initial nuclear alignment $\alpha_2 = 0.53 \pm 0.05$. The solution for the mixing ratio of the $(E2/M1)$ transition to the 2814-keV state is then given by $-2.3 < x < -0.65$. The previous measurement of Lopes *et al.*[7] gave $-1.2 < x < -0.5$, in very good agreement with our result. From the measured lifetime and assuming $|x| = 0.92$ we compute $E2$ and $M1$ transition strengths of 1.3 ± 0.3 W.u. and $(3.0 \pm 0.7) \times 10^{-4}$ W.u., respectively, for the decay to the 2814-keV level The rigorous upper limit on the $M1$ transition strength (corresponding to $x = 0$) is 8×10^{-4} W.u., where we have allowed for two standard deviations in the measured lifetime.

C. Decay of the 3944-keV level

This level is one member of a close-lying doublet with states at 3939 and 3944 keV.[12] The lifetime of the lower member, which was not populated in the present experiment, has been measured[8,12] to be 95 ± 25 fs. A mean life of 1.2 ± 0.4 ps has been quoted[12] for the 3944-keV state, which decays via 347- and 1130-keV γ rays to the 3598- and 2814-keV states, respectively. We have determined the lifetime of the 3944-keV state from recoil-distance measurements on both of these γ rays (Fig. 9), and we find a value of 16.1 ± 1.6 ps in strong disagreement with Ref. 12. The stopped and shifted peaks for the 1130-keV transition are particularly clean (Fig. 7), and the γ-γ coincidence data show no evidence of strong feeding from long-lived states. We conclude that the mean life of the 3944-keV level is substantially longer than indicated by previous Doppler-shift attenuation measurements.

The branching ratios for the decay of the 3944-keV level to the 3598- and 2814-keV states are 0.36 ± 0.05 and 0.64 ± 0.05, respectively. These results, which have been corrected for the angular distribution of the γ radiation, are not in good agreement with the values 0.47 ± 0.03 and 0.53 ± 0.03 quoted in Ref. 12. From our results for the lifetime of the 3944-keV state and its branching ratio to the $\frac{7}{2}^-$ state at 2814 keV, we compute a strength of 2.2 ± 0.3 W.u. if this transition is $E2$. In this case, the probability of a measurable $M3$ admixture is negligible (a 10% effect on a_2 requires a 2×10^4 W.u. $M3$ transition) so we assume $x = 0$. In addition, the maximum allowable $(E2/M1)$ mixing ratio (corresponding to a 100 W.u. $E2$ transition[20]) for the decay to the 3598-keV state is $|x| \leq 0.53$. These limits were used in the determination of a spin-parity assignment for the 3944-keV level from the angular distributions of the 347- and 1130-keV γ rays (Fig. 5). We consider spin assignments of $(\frac{7}{2}, \frac{9}{2}, \frac{11}{2})$ for the 3944-keV state since, as noted above, the 347-keV transition to the $\frac{9}{2}^-$ state at 3598 keV must be at least partially dipole. All three possibilities are allowed if no restriction is placed on the magnetic substate populations. If, however, we require $\alpha_K > 0$, then the $J = \frac{9}{2}$ assignment is rejected at well above the 0.1% confidence limit. For the $J = \frac{11}{2}$ alternative we can use the a_2 coefficient (Table II) for the 1130-keV γ ray to determine the alignment $\alpha_2 = 0.51 \pm 0.05$. The solutions for the mixing ratio of the $(E2/M1)$ transition to the $\frac{9}{2}^-$ state at 3598 keV are $x = 0.16 \pm 0.02$ and $x = 3.2 \pm 0.3$. The latter value, however, is rejected since it requires an $E2$ transition of over 400 W.u.[20] Assuming $x = 0.16$, we compute $E2$ and $M1$ transition strengths of 8.9 ± 1.5 W.u. and $(1.6 \pm 0.3) \times 10^{-2}$ W.u., respectively, for the 347-keV transition. The upper limit for the $M1$ transition strength (corresponding to $x = 0$) is 2.3×10^{-2} W.u. The parity of this state is odd if $J = \frac{11}{2}$ since the required $M2$ transition strengths for the decays to the $\frac{9}{2}^-$ and $\frac{7}{2}^-$ states are too large to allow positive parity.[20] Finally, the $J = \frac{7}{2}$ possibility gives fits to the angular distributions for a wide range of acceptable mixing ratios for the two transitions. We consider the $J = \frac{7}{2}$ possibility to be remote, however, since it is a feature of both the heavy-ion reaction model[1] and empirical observation[13] that high-spin states, and more specifically the lowest levels of a given J (yrast levels[1]), are the most strongly populated in these reactions. The 3944-keV state is by far the state most strongly fed in this reaction (Fig. 4). This argument is circumstantial, however, so that the $J^\pi = (\frac{11}{2}^-)$ assignment to the 3944-keV state should be regarded as a working hypothesis.

D. Decay of the 5719- and 6476-keV states

The ordering of the two highest-energy states inferred from the present experiments is somewhat open to question since crossover transitions have not been observed for either of them. The

ordering could be determined from the relative intensities of the two γ rays if there were appreciable side feeding of the lower state, but this is not the case, as shown in Fig. 4. We originally chose to place the intermediate state at 5719-keV because a level has been observed at about this energy in previous experiments.[9] During the course of this experiment, we became aware of the work of Alenius, Arnell, and Stankiewicz[21] who place the transitions in the same order.

The 5719-keV state decays via a 1775-keV γ transition to the 3944-keV level. We obtained 2.7 ± 1.5 ps for the mean life of this transition which, with the assumption of $J^\pi = \frac{11}{2}^-$ for the 3944-keV state, rigorously limits the spin of the 5719-keV level to $J = (\frac{7}{2} - \frac{15}{2})$. If we now assume $\alpha_K > 0$ and use the measured mean life to limit the possible contribution of octupole radiation,[20] the measured angular distribution is only consistent with $J = (\frac{9}{2}, \frac{13}{2})$. No direct feeding of the 5719-keV state is observed in this reaction (Fig. 4), but instead the 5719-keV level is fed via the 757-keV transition from the 6476-keV state. In the absence of side feeding it is possible to fit the 757- and the 1774-keV transitions simultaneously. When this is done, the minimum allowable value for the mixing ratio of the 1774-keV transition is $|x| \geq 1.5$, which rules out[20] positive parity for the 5719-keV state since a 56-W.u. $M2$ transition is required. The $M1$ and $E2$ transition strengths for the decay to the 3944-keV level (Table III) are all reasonable values for transition strengths in this mass region.[20]

The lifetime of the 6476-keV state is shorter than that of the 5719-keV state, but it is also long enough so that the 757-keV γ ray is not noticeably Doppler shifted. Therefore it must be of the order of 1 ps. This lifetime is short enough so that the 757-keV transition must be at least partially dipole, since the single-particle $E2$ mean life is 408 ps. This rigorously limits the spin of the 6476-keV level to $J = (\frac{7}{2} - \frac{11}{2})$ if the 5719-keV state is $J = \frac{9}{2}$, and to $J = (\frac{11}{2} - \frac{15}{2})$ if the 5719-keV level has $J = \frac{13}{2}$. If we now make the model assumption $\alpha_K > 0$, the $J \rightarrow J$ possibility is ruled out in both cases. The mixing ratio for the $6476 \rightarrow 5719$ transition from a simultaneous fit to the angular distributions of the 757- and 1774-keV γ rays is limited by $-0.27 \leq x \leq 0.10$ for all possible spin combinations for the two levels, which suggests a nearly pure dipole transition with an $E1$ strength of $\sim 2 \times 10^{-3}$ W.u. or an $M1$ strength of $\sim 7 \times 10^{-2}$ W.u. Both of these are reasonable values[20] so the parity of this state cannot be determined. Finally, the fact that the 6476-keV state is directly fed with a rather large intensity in this reaction (Fig. 4) suggests that it has high spin, so that we consider the $J = \frac{7}{2}$ possibility to be remote and assign $J = (\frac{11}{2}, \frac{15}{2})$ to the 6476-keV state.

IV. CONCLUSION

The electromagnetic decay modes of five high-spin states in ^{39}K have been investigated by means of the ^{24}Mg(^{18}O, $p2n\gamma\gamma\cdots$)^{39}K reaction. The information obtained from this experiment clearly illustrates the power of these heavy-ion-induced compound-nuclear reactions in the nuclear spectroscopy of high-spin states. In particular, we have obtained spin-parity assignments for these ^{39}K states, and also the multipole mixing ratios and electromagnetic matrix elements for their γ decays. It must be recognized that most of these results are not based on rigorous arguments but are only strongly circumstantial because they depend to some extent on a reaction model, and one which is not as yet thoroughly investigated. We note, however, that identical reaction-dependent arguments have long been employed in heavier mass regions.[1] It is to be hoped that a systematic survey of heavy-ion compound-nucleus reactions leading to upper s-d-shell and $f_{7/2}$-shell nuclei, such as we have undertaken, will provide additional evidence on the applicability of these arguments to lighter systems. Such a study would greatly benefit from investigations of those high-spin states which can be reached via reactions such as (α, t) in a collinear geometry which would allow more rigorous determination of substate populations. Generally, these will only be the lowest few (both in energy and angular momentum) of the states seen in heavy-ion reactions. Nevertheless, they will provide a firm starting point for further investigations.

Some intriguing questions have also been raised from this experiment. First of all, the $M1$ transition strengths observed in ^{39}K are rather small. The average value of the three $M1$ transition strengths is 6×10^{-3} W.u. which is quite weak for normal $M1$ transitions in this mass region. It would be interesting to see if the cancellations in the $M1$ amplitudes are physically meaningful or only accidental. Also it appears probable that the 6476-keV state might have spin $J = \frac{15}{2}$, which cannot be made from the simple particle-hole excitation which is the basis of most shell-model calculations.[4] If this is the case, the parity of this state is extremely interesting since it may give a good deal of information on the shell structure of ^{39}K. Finally, the behavior of the single-α-out excitation function (Fig. 2) is surely of interest and should be further investigated with particle-γ coincidence techniques.

Note added in proof: The linear polarizations of the seven ^{39}K γ rays discussed in this paper have recently been measured at BNL with the Johns Hopkins polarimeter.[22] Using the analysis of the γ-ray angular distributions presented above, together with the known positive parity of the ^{39}K ground state,[11] we can assign negative parity to all of the ^{39}K states mentioned above except for the 6476-keV level which has positive parity. The required mixing ratios are also consistent with those presented in Table III.[23]

---

†Work performed under the auspices of the U. S. Atomic Energy Commission.

*On leave from Laboratoire Spectrométrie Nucléaire, Strasbourg, France.

‡Guest physicist. Permanent address: University of Auckland, Auckland, New Zealand.

[1]J. O. Newton, Prog. Nucl. Phys. 11, 53 (1970); Oak Ridge National Laboratory Report No. CONF-720669, 1973 (unpublished).

[2]T. Nomura, H. Morinaga, and B. Povh, Nucl. Phys. A127, 1 (1969).

[3]F. C. Erné, Nucl. Phys. 84, 91 (1966).

[4]S. Maripuu and G. A. Hokken, Nucl. Phys. A141, 481 (1970).

[5]M. B. Lewis, Phys. Lett. 27B, 13 (1968); M. B. Lewis, N. R. Roberson, and D. R. Tilley, Phys. Rev. 168, 1205 (1968).

[6]P. Goode and L. Zamick, Nucl. Phys. A129, 81 (1969).

[7]J. S. Lopes, B. C. Robertson, R. D. Gill, R. A. I. Bell, and H. J. Rose, Nucl. Phys. A109, 241 (1968).

[8]R. M. Tapphorn, M. Kregar, and G. G. Seaman, Phys. Rev. C 3, 2232 (1971).

[9]P. D. Bond and B. D. Kern, Phys. Rev. C 6, 873 (1972).

[10]W. Kessel, R. Bass, and R. Wechsung, Nucl. Phys. A206, 193 (1973).

[11]P. M. Endt and C. Van der Leun, Nucl. Phys. A214, 1 (1973).

[12]J. L. Durell, V. Metag, R. Repnow, A. N. James, J. F. Sharpey-Schafer, and P. von Brentano, Phys. Rev. Lett. 28, 1723 (1972).

[13]Ph. Gorodetzky, J. J. Kolata, J. W. Olness, A. R. Poletti, and E. K. Warburton, Phys. Rev. Lett. 31, 1067 (1973).

[14]D. B. Fossan and E. K. Warburton, in Nuclear Spectroscopy, edited by J. Cerny (Academic, New York, to be published).

[15]K. W. Jones, A. Z. Schwarzschild, E. K. Warburton, and D. B. Fossan, Phys. Rev. 178, 1773 (1969).

[16]R. M. Diamond, E. Matthias, J. O. Newton, and F. S. Stephens, Phys. Rev. Lett. 16, 1205 (1966).

[17]P. D. Bond, private communication.

[18]A. R. Poletti and E. K. Warburton, Phys. Rev. 137, B595 (1965).

[19]T. Yamazaki, Nucl. Data A3, 1 (1967).

[20]P. M. Endt and C. Van der Leun, to be published.

[21]N. G. Alenius, S. E. Arnell, and O. Stankiewicz, in Stockholm 80-cm Cyclotron Progress Report, 1972 (unpublished).

[22]J. S. Kim and Y. K. Lee, The Johns Hopkins University Atomic Energy Report No. COO-3274-8, 1973 (unpublished).

[23]E. Beardsworth, J. S. Kim, J. J. Kolata, A. H. Lumpkin, J. W. Olness, and E. K. Warburton, to be published.